Calculation of the G-Tensor of Electron Paramagnetic Resonance Spectroscopy Using Gauge-Including Atomic Orbitals and Density Functional Theory

Georg Schreckenbach and Tom Ziegler*

Department of Chemistry, The University of Calgary, Calgary, Alberta, Canada T2N 1N4

Received: October 4, 1996; In Final Form: December 30, 1996[⊗]

An implementation of the *g*-tensor of electron paramagnetic resonance (EPR) spectroscopy is presented. This implementation is based on density functional theory (DFT) and the use of gauge-including atomic orbitals (GIAO). Contributions from the spin−other-orbit operators are neglected, while all the other relevant perturbation operators are included. The new method is an extension of an existing DFT−GIAO program package for the calculation of the chemical shift of nuclear magnetic resonance spectroscopy; full use is made of the conceptual analogy between the *g*-tensor and the chemical shift. The new program is applied to various small radicals. The agreement of calculated and experimental *g*-tensors is good for radicals of first-row elements; experimental trends are generally well reproduced. The quality of calculated results is worse if the scheme is applied to compounds of heavier elements. Possible reasons for these apparent shortcomings of the method are discussed.

1. Introduction

Magnetic resonance spectroscopy comprises some of the most powerful and versatile analytic tools available to date. Nuclear magnetic resonance (NMR) spectroscopy[1,2] is mostly useful for closed shell systems with vanishing electron spin magnetic moment, while electron paramagnetic resonance (EPR) spectroscopy[3−6] is generally being applied to radicals and transition metal complexes.

The *g*-tensor is an important part of any EPR spectrum. It can provide information about the radical species present. Further, conclusions regarding conformation, electronic structure, and other properties are often sought.[3−10] It would thus be desirable to determine the *g*-tensor of a given molecule from electronic structure calculations. This would allow us to enhance our understanding of electronic factors governing the observed spectra. Further, such calculations could be used to identify unstable radicals from their spectra and accompanying calculations of possible candidates.[11] Various other applications are easily conceivable.

Semiempirical calculations of the *g*-tensor have been around for a long time (they are summarized in textbooks like, *e.g.*, chapter 15 in the book by A. Abragam and B. Bleaney[9]). G. Lushington has reviewed them in chapter 1 of his Ph.D. thesis.[12] Articles on *ab initio* calculations exist in the literature as well. However, these Hartree−Fock-based calculations are comparatively rare and most of them are at least 15 years old. Consequently, they are restricted by very small basis sets. None of them accounts for all of the relevant perturbation operators. These calculations[13−18] have been reviewed by Lushington as well.[12]

The mentioned Ph.D. thesis by Lushington,[12] along with related papers,[19−22] affords the first modern *ab initio* implementation of the *g*-tensor. Lushington's work comprises the complete treatment of all relevant terms at the Hartree−Fock level of theory[12,19−22] and a correlated multireference configuration interaction (MRCI) extension.[12,22] We will compare our results to this pioneering and promising work later.

To the best of our knowledge, there is no first principle method available for the calculation of the *g*-tensor that employs density functional theory (DFT). Neither is there any formulation available that is based on the use of "gauge-including atomic orbitals" (GIAO)[23,24] or other distributed-origin schemes. Given the importance of this spectroscopic property and the success of DFT for other magnetic properties,[25−34] it seems timely to fill the gap. The calculation of the *g*-tensor based on density functional theory (DFT) is the subject of the present paper.[31] Recently, there has been a strong interest in the calculation of the NMR shielding tensor based on DFT.[25−34] Given the close theoretical connection between the EPR *g*-tensor and the NMR shielding tensor, see below, it is possible to extend our existing DFT−NMR program[28−32] to the EPR case.

Our DFT−NMR program[28] is based on the use of GIAOs. Other calculations of the *g*-tensor are based on the use of a common gauge origin for the whole system.[12] They may thus be prone to the so-called gauge problem, *i.e.*, the dependence of the results on the arbitrary coordinate origin. The gauge problem is well-known for the NMR shielding.[2,35−37] Lushington discussed the gauge dependence of his results in detail.[12]

Earlier, we have extended the DFT−GIAO−NMR scheme to include the frozen core approximation,[29] as well as scalar relativity.[30] Further, a detailed analysis in terms of the molecular orbitals is available.[38,39] All of these features are readily transferable to the EPR *g*-tensor as well. This constitutes a major advantage of the formulation that we are presenting here.

2. Theory

2.1. Perturbation Operators. The *g*-tensor of EPR spectroscopy can be considered as a second-order property.[40,41] The perturbation parameters are in this case one Cartesian component of the constant external magnetic field, B_s and the net electronic spin component along a given coordinate axis, S_t. The *st* tensor component of $\vec{\vec{g}}$ is then given by[4]

$$g_{st} = \frac{1}{\mu_B} \frac{\partial^2 E}{\partial B_s \partial S_t}\bigg|_{\vec{B}=\vec{S}=0} \tag{1}$$

Here, E is the total energy of the many-electron system. Further, μ_B is the Bohr magneton and μ_B equals $\alpha/2$ in atomic units, where α is the dimensionless fine structure constant, given as

[⊗] Abstract published in *Advance ACS Abstracts,* February 15, 1997.

S1089-5639(96)03060-5 CCC: $14.00

1/137.03599.[42] All the derivations in this paper will be based on atomic units.[4]

It follows from eq 1 and from the interchange theorem of double-perturbation theory[40,41,43−45] that we have to calculate the electronic wave function up to first order in in one of the perturbations alone. If we chose the external magnetic field, then this task is the same as that for the NMR shielding.[28−31] Alternatively, it would be possible to calculate the electronic wave function up to first order in the electronic spin — but in this case, the analogy with the formulation of the NMR shielding would be lost. It is further clear from eq 1 that only such perturbation operators are needed that are either linear in the electronic spin operator, yielding paramagnetic contributions, or bilinear in both, the external magnetic field and the spin operator. The latter operators are responsible for diamagnetic contributions. All of these perturbation operators will be given next.

The relevant perturbation Hamiltonian can be obtained from relativistic many-body quantum mechanics. Usually, the nonrelativistic limit is taken, resulting in various perturbation operators. These operators are listed in textbooks[4,41,46] and in review articles (*e.g.*, ref 47). Possibly the best, most comprehensive, and most accurate account is given in Harriman's book.[4]

The operators that are relevant for the EPR *g*-tensor include:[4,41,46] the electron spin Zeeman operator

$$h_{\mathrm{Z}} = \frac{\alpha}{2} g_{\mathrm{e}} \vec{S}\cdot\vec{B} \tag{2}$$

the kinetic energy correction to the electron spin Zeeman operator

$$h_{\mathrm{Z-KE}} = -\frac{\alpha^3 g_{\mathrm{e}}}{4} p^2 \vec{S}\cdot\vec{B} \tag{3}$$

the (electron−nuclear) spin−orbit operator

$$h_{\mathrm{SO-N}} = \frac{\alpha^2 g'}{4} \sum_{A}^{N_{\mathrm{NUC}}} \sum_{j}^{n} \vec{S}_j \cdot \left[\frac{Z_A}{|r_j - R_A|^3} (\vec{r}_j - \vec{R}_A) \times \vec{p}_j \right] \tag{4}$$

the electron−electron spin−orbit operator

$$h_{\mathrm{SO-e}} = -\frac{\alpha^2 g'}{4} {\sum_{j,k}^{n}}' \vec{S}_j \cdot \left[\frac{\vec{r}_j - \vec{r}_k}{|\vec{r}_j - \vec{r}_k|^3} \times \vec{p}_j \right] \tag{5}$$

the spin−other-orbit operator

$$h_{\mathrm{SOO}} = -\alpha^2 {\sum_{j,k}^{n}}' \vec{S}_j \cdot \left[\frac{\vec{r}_k - \vec{r}_j}{|\vec{r}_k - \vec{r}_j|^3} \times \vec{p}_k \right] \tag{6}$$

and finally the diamagnetic correction terms to $h_{\mathrm{SO-N}}$, $h_{\mathrm{SO-e}}$, and h_{SOO}, respectively,

$$h^{\mathrm{dia}}_{\mathrm{SO-N}} = \frac{\alpha^3 g'}{8} \sum_{A}^{N_{\mathrm{NUC}}} \sum_{j}^{n} \frac{Z_A}{|r_j - R_A|^3} \{ [(\vec{r}_j - \vec{R}_A)\cdot\vec{r}_j](\vec{S}_j\cdot\vec{B}) - (\vec{S}_j\cdot\vec{r}_j)[(\vec{r}_j - \vec{R}_A)\cdot\vec{B}] \} \tag{7}$$

$$h^{\mathrm{dia}}_{\mathrm{SO-e}} = -\frac{\alpha^3 g'}{8} {\sum_{j,k}^{n}}' \frac{1}{|\vec{r}_j - \vec{r}_k|^3} \{ [(\vec{r}_k - \vec{r}_j)\cdot\vec{r}_j](\vec{S}_j\cdot\vec{B}) - (\vec{S}_j\cdot\vec{r}_j)[(\vec{r}_k - \vec{r}_j)\cdot\vec{B}] \} \tag{8}$$

and

$$h^{\mathrm{dia}}_{\mathrm{SOO}} = -\frac{\alpha^3}{2} {\sum_{j,k}^{n}}' \frac{1}{|\vec{r}_j - \vec{r}_k|^3} \{ [(\vec{r}_j - \vec{r}_k)\cdot\vec{r}_k](\vec{S}_j\cdot\vec{B}) - (\vec{S}_j\cdot\vec{r}_k)[(\vec{r}_j - \vec{r}_k)\cdot\vec{B}] \} \tag{9}$$

The last three terms are titled "gauge correction terms" in Harriman's book[4] and other sources;[12] we chose the name "diamagnetic terms" because of their analogy with the operators of the diamagnetic NMR shielding.[28] In eqs 2−9, we use the following notation: $\vec{p}_j$, $\vec{S}_j$, and $\vec{r}_j$ are the momentum, spin, and position operators for electron *j*,

$$\vec{S} = \sum_{j}^{n} \vec{S}_j \tag{10}$$

Further, Z_A is the charge of nucleus A. The total number of nuclei is N_{NUC} while the total number of electrons is *n*. The double summations over *j* and *k* in eqs 5, 6, 8, and 9 exclude the case where $j = k$. Finally, g_{e} is the electronic Zeeman *g*-factor, and g' is the electronic spin−orbit *g*-factor.[4] They are given by[3,4]

$$g_{\mathrm{e}} = 2.002\ 319\ 277\ 8 \tag{11a}$$

and

$$g' = 2.004\ 638\ 555\ 6 \tag{11b}$$

or[4]

$$\mathrm{g}' = 2(1 + 2g_1) \tag{11c}$$

where

$$g_1 = \frac{1}{2}(g_{\mathrm{e}} - 2) \tag{11d}$$

Harriman points out that, although g_{e} and g' are certainly appropriate in h_{Z} and $h_{\mathrm{SO-e}}$, respectively, "*the treatment of radiative corrections* [in the derivation of these terms] *has been incomplete so great significance should not be attached to the distinction between* g_e, g', *and 2 in higher orders*" (cited from ref 4, p. 378). Note that the spin−other-orbit operators, eqs 6 and 9, contain neither g_{e} nor g'. In the literature, there are also other values for g_{e} that differ from the one cited in eq 11a.[3,4,12,46,48] The differences show up only in the last few digits and have no influence on the numbers that will be cited in this paper.

The diamagnetic operators in eqs 7−9 contain both the electronic spin operator and the magnetic field. According to eq 1, they have to be used with the zero-order, unperturbed wave function. Note that the diamagnetic operators follow from their field free counterparts $h_{\mathrm{SO-N}}$, $h_{\mathrm{SO-e}}$, and h_{SOO}, respectively, by means of the so-called minimal coupling.[41,46,49] Minimal coupling is a general procedure to introduce the magnetic field into field free expressions. In this scheme, we substitute the electronic momentum operator $\vec{p}$ according to

$$\vec{p} \xrightarrow{\text{substitute}} \vec{p} + \alpha\vec{A} \tag{12}$$

where $\vec{A}$ represents the vector potential of the constant external magnetic field.[50]

The nuclear spin−orbit operator, $h_{\mathrm{SO-N}}$ of eq 4, and its diamagnetic counterpart, $h^{\mathrm{dia}}_{\mathrm{SO-N}}$ of eq 7, can be reformulated in

terms of the nuclear potential V_N of the N_{NUC} nuclei in the system

$$V_N(\vec{r}) = -\sum_{N_{NUC}}^{A} \frac{Z_A}{|r - R_A|} \tag{13}$$

We obtain for h_{SO-N} and h_{SO-N}^{dia}

$$h_{SO-N} = \frac{\alpha^2 g'}{4} \sum_j^n \vec{S}_j \cdot \left[\frac{\partial V_N}{\partial \vec{r}} \times \vec{p}_j \right] \tag{14}$$

and

$$h_{SO-N}^{dia} = \frac{\alpha^3 g'}{8} \sum_j^n \left\{ \left[\frac{\partial V_N}{\partial \vec{r}} \cdot \vec{r}_j \right] (\vec{S}_j \cdot \vec{B}) - (\vec{S}_j \cdot \vec{r}_j) \left[\frac{\partial V_N}{\partial \vec{r}} \cdot \vec{B} \right] \right\} \tag{15}$$

The electronic spin−orbit operator, h_{SO-e} of eq 5, and its diamagnetic counterpart, h_{SO-e}^{dia} of eq 8, can be reformulated in a similar way, using the electrostatic potential of the other electrons in the system instead of the nuclear potential, V_N of eq 13.

2.2. G-Shifts. We define the *g*-shift Δg as the deviation of the molecular *g*-value from the free electron value g_e[12]

$$\vec{\vec{g}} = g_e \vec{\vec{1}} + \Delta \vec{\vec{g}} \tag{16}$$

Here, $\vec{\vec{1}}$ is the unit tensor. Note that both $\vec{\vec{g}}$ and $\Delta\vec{\vec{g}}$ are second-rank tensors. The isotropic *g*-shift Δg is the trace of $\Delta\vec{\vec{g}}$. There is also an alternative definition used in the literature, *e.g.*, in Atkins' textbook:[48]

$$\vec{\vec{g}} = g_e(\vec{\vec{1}} - \tilde{\Delta}\vec{\vec{g}}) \tag{17}$$

This latter definition has the advantage that $\tilde{\Delta}\vec{\vec{g}}$ has the same sign convention as the NMR shielding $\vec{\vec{\sigma}}$.[36,37] However, the former definition seems to be more common, and we employ exclusively Δg (or $\Delta\vec{\vec{g}}$) throughout the present paper.

The Zeeman operator, eq 2, results in the isotropic free electron *g*-value g_e. Thus, it doesn't contribute to the *g*-shift Δg, according to eq 16. The remaining perturbations (eqs 3−9) contribute, however, to Δg. We shall discuss these contributions in more detail now.

2.3. G-Tensor within Density Functional Theory. We will evaluate the Δg-tensor, eqs 1 and 16, within the framework of density functional theory (DFT).[51−56]

We have seen in eqs 14 and 15 that the spin−orbit terms h_{SO-N} and h_{SO-N}^{dia}, respectively, can be written as the interaction of the electronic spin with the potential in which the electrons are moving, the movement being represented by the momentum operator $\vec{p}$. Further, in DFT, the electrons are thought to move in an effective potential that is due to the other electrons and the nuclei.[51] It is thus justified to replace the nuclear potential V_N of eq 13 by an effective potential. The form of this effective potential will be specified shortly. It would be the effective potential that is experienced by the electrons; we would substitute V_N in the spin−orbit operators h_{SO-N} and h_{SO-N}^{dia}:

$$h_{SO} = \frac{\alpha^2 g'}{4} \vec{S} \cdot \left(\frac{\partial V_{eff}}{\partial \vec{r}} \times \vec{p} \right) \tag{18}$$

and

$$h_{SO}^{dia} = \frac{\alpha^3 g'}{8} \sum_j^n \left\{ \left[\frac{\partial V_{eff}}{\partial \vec{r}} \cdot \vec{r}_j \right] (\vec{S}_j \cdot \vec{B}) - (\vec{S}_j \cdot \vec{r}_j) \left[\frac{\partial V_{eff}}{\partial \vec{r}} \cdot \vec{B} \right] \right\} \tag{19}$$

In this way, we incorporate the interaction of the electronic spin with both, the external, nuclear potential *and* the potential due to the other electrons. Thus, we have accounted for both the nuclear and electronic spin−orbit terms by including an effective potential V_{eff} into eqs 18 and 19. As pointed out above, V_{eff} should contain the nuclear potential, V_N of eq 13, and the potential due to the other electrons in the system. We can use the Coulomb potential V_C for the electronic part. This potential is the electrostatic potential of the total electronic density ρ of the system and is given by

$$V_C(\rho, \vec{r}_1) = \int d\vec{r}_2 \frac{\rho(\vec{r}_2)}{|\vec{r}_1 - \vec{r}_2|} \tag{20}$$

However, the use of V_C introduces an error, since V_C is the average potential due to the total electronic density, *i.e.*, due to *all* electrons in the system. We will remove this error by including an approximate exchange potential into the effective potential. This is possible since exchange potentials correct for the mentioned error.[51] The effective potential V_{eff} is thus given by[57−60]

$$V_{eff} = V_N + V_C + V_{X\alpha} \tag{21}$$

Here, we have used the simplest possible functional form of an exchange potential, the X_α potential.[51,61]

In summary, we have accurately accounted for the operators h_{SO-N} and h_{SO-N}^{dia}, eqs 14 and 15, with the formulation that is expressed in eqs 19−21. We have further included the electronic spin−orbit contributions of eqs 5 and 8 in an approximate way. However, the spin−other-orbit contributions, eqs 6 and 9, respectively, have been neglected. This deserves some further discussion. We assume it to be a good approximation because contributions from the spin−other-orbit terms are probably small. It can be shown that these contributions vanish exactly for a model system containing one unpaired electron together with a closed shell system of other electrons. In real systems with one unpaired electron, there will be some spin polarization of the lower shells. This results in (presumably small) contributions to the *g*-tensor from the spin−other-orbit operators. The neglect of these contributions seems to be justified. The only case where the spin−other-orbit operators *might* be significant is in systems with more than one unpaired electron. In physical terms, we consider the reference electron as moving in a *static* electron cloud that is due to the other electrons in the molecule. We will briefly come back to the discussion of the spin−other-orbit terms later in the conclusions.

2.4. Evaluation of the Δg-Tensor. In the previous section, we have derived a form of the spin−orbit operators that can be evaluated based on double-perturbation theory[40] and DFT. This requires to treat the expression in eq 1 further. This task is, however, not entirely trivial since both the magnetic field $\vec{B}$ and the electronic spin $\vec{S}$ of eq 10 are quantum-mechanical operators. The necessary procedure is called "spin-field reduction".[12,41] Thus, the direction of the magnetic field determines the axis of spin quantization.[41] An expectation value of some one-electron operator $\hat{O} \cdot S_z$ that is proportional to the z-

component S_z of the spin operator can be written as

$$\langle\Psi|\hat{O}\cdot S_z|\Psi\rangle = \int_{\vec{r}\to\vec{r}} d\tau\, \hat{O}\rho^{\alpha}(\vec{r},\vec{r}') - \int_{\vec{r}\to\vec{r}'} d\tau\, \hat{O}\rho^{\beta}(\vec{r},\vec{r}') \quad (22)$$

In eq 22, we have introduced the density matrices of the α and β electrons,

$$\rho^{\tau}(\vec{r},\vec{r}') = \sum_{i}^{n_\tau} \Psi_i^{\tau}(\vec{r})\Psi_i^{\tau}(\vec{r}'), \quad \tau = \alpha,\beta \quad (23)$$

where n_α and n_β are the numbers of electrons with α and β spins, respectively

$$n_\alpha + n_\beta = n \quad (24)$$

The total number of electrons is n. The total electronic density $\rho(\vec{r})$ follows from the density matrices (eq 23) by

$$\rho(\vec{r}) = \rho(\vec{r},\vec{r}) \quad (25a)$$

$$\rho(\vec{r},\vec{r}') = \rho^{\alpha}(\vec{r},\vec{r}') + \rho^{\beta}(\vec{r},\vec{r}') \quad (25b)$$

or

$$\rho(\vec{r},\vec{r}') = \sum_{i}^{n} \Psi_i(\vec{r})\Psi_i(\vec{r}') \quad (26)$$

The $\{\Psi_i\}$ (eq 26) form a set of n one-electron functions; in DFT, they are usually called the Kohn−Sham orbitals.[51,62,63]

With this formalism, we get from eq 1 for the *st* component of the *g*-shift $\Delta\vec{\vec{g}}$:

$$\Delta g_{st} = \frac{\partial}{\partial B_s}\{\int_{\vec{r}\to\vec{r}'} d\tau (h_t^{01,\mathrm{EPR}} + \sum_{r=1}^{3} B_r h_{rt}^{11,\mathrm{EPR}}) \times [\rho^{\alpha}(\vec{B}|\vec{r},\vec{r}') - \rho^{\beta}(\vec{B}|\vec{r},\vec{r}')]\}_{\vec{B}=0} \quad (27)$$

This expression was based on the aforementioned interchange theorem of double-perturbation theory.[40,41,43−45] Here $\rho^{\alpha}(\vec{B}|\vec{r},\vec{r}')$ and $\rho^{\beta}(\vec{B}|\vec{r},\vec{r}')$ are the ground state electronic density matrices of eq 23 under the influence of the external magnetic field.[28−31] The factor $1/\mu_B$ of eq 1 is absorbed by the operators in eq 27. These operators are $h_t^{01,\mathrm{EPR}}$ and $h_{st}^{11,\mathrm{EPR}}$; they follow from the previous section. We find for $h_t^{01,\mathrm{EPR}}$ (cf eq 18)

$$h_t^{01,\mathrm{EPR}} = \frac{1}{\mu_B}\frac{\partial h_{\mathrm{SO}}}{\partial S_t}\bigg|_{\vec{S}=0} \quad (28a)$$

$$= \frac{\alpha i g'}{2}\left(\frac{\partial V_{\mathrm{eff}}}{\partial \vec{r}} \times \vec{p}\right)_t \quad (28b)$$

Similarly, we have for the diamagnetic operator $h_{st}^{11,\mathrm{EPR}}$:

$$h_{st}^{11,\mathrm{EPR}} = \frac{1}{\mu_B}\frac{\partial^2 H}{\partial B_s \partial S_t}\bigg|_{\vec{B}=0\,\vec{S}=0} \quad (29a)$$

where H is the Kohn−Sham one-electron operator of the system including the magnetic field and the electronic spin. The factor $1/\mu_B$ has been absorbed again by the operator as mentioned above. The operator $h_{st}^{11,\mathrm{EPR}}$ contains terms that are bilinear in the magnetic field and the spin magnetic moment. Such operators include the Zeeman operator proper, eq 2, the kinetic energy correction to the Zeeman operator, eq 3, and the diamagnetic spin−orbit operators. We will use the latter in the form that has been derived in eq 19. The diamagnetic spin−other-orbit operator, eq 9, is also of this form. We will neglect it, however, according to the discussion above. The Zeeman operator of eq 2 will not contribute to $h_{st}^{11,\mathrm{EPR}}$, based on the definition of $\Delta\vec{\vec{g}}$ in eq 16. We are therefore left with the following expression for $h_{st}^{11,\mathrm{EPR}}$:

$$h_{st}^{11,\mathrm{EPR}} = h_{st}^{11,\mathrm{KE}} + h_{st}^{11,\mathrm{SO}} \quad (29b)$$

where

$$h_{st}^{11,\mathrm{KE}} = -\frac{\alpha^2 g_e}{2} p^2 \delta_{st} \quad (29c)$$

and

$$h_{st}^{11,\mathrm{SO}} = \frac{\alpha^2 g'}{4}\left\{\frac{\partial V_{\mathrm{eff}}}{\partial \vec{r}}\cdot\vec{r}\,\delta_{st} - \left(\frac{\partial V_{\mathrm{eff}}}{\partial \vec{r}}\right)_s r_t\right\} \quad (29d)$$

The expressions in eqs 27 to 29 can be evaluated with the apparatus that had been developed for the NMR shielding tensor.[28−31] This is, in some more detail, the subject of the next section.

3. Implementation of the EPR Δ*g*-Tensor into the DFT−GIAO Program; Working Equations

The expressions in eqs 27 to 29 will be evaluated on the basis of our NMR−DFT−GIAO program.[28−31] We are able to do that since $\Delta\vec{\vec{g}}$ relies on the first-order magnetic density matrix, eq 27, as does the NMR shielding tensor.[28−32] The analogy between the two properties is, however, not exhausted with the first order magnetic density matrix. This becomes apparent by noting the similarity between the para- and diamagnetic operators of the NMR case[28] and the respective EPR operators, $h_t^{01,\mathrm{EPR}}$ and $h_{st}^{11,\mathrm{SO}}$ of eqs 28b and 29d. We had in the NMR case[28]

$$h_t^{01,\mathrm{NMR}} = \alpha i\left[\frac{\vec{r}_N}{r_N^3} \times \vec{p}\right]_t \quad (30)$$

and

$$h_{st}^{11,\mathrm{NMR}} = \frac{\alpha^2}{2r_N^3}[\vec{r}_N\cdot\vec{r}\,\delta_{st} - r_{N_s} r_t] \quad (31)$$

Thus, we obtain the EPR operators from $h_t^{01,\mathrm{NMR}}$ and $h_{st}^{11,\mathrm{NMR}}$ by the simple substitution

$$\frac{\vec{r}_N}{r_N^3} \xrightarrow{\text{substitute}} \frac{g'}{2}\frac{\partial V_{\mathrm{eff}}}{\partial \vec{r}} \quad (32)$$

(NMR case) (EPR case)

Using this analogy, we find the following working equations for the *g*-shift $\Delta\vec{\vec{g}}$ (*st* tensor component):

$$\Delta g_{st} = \Delta g_{st}^{\mathrm{KE}} + \Delta g_{st}^{\mathrm{d}} + \Delta g_{st}^{\mathrm{p}} \quad (33)$$

The different contributions in eq 33 are due, in this order, to the Zeeman kinetic energy correction, eq 29c, the diamagnetic spin−orbit operator, $h_{st}^{11,\mathrm{SO}}$ of eq 29d, and the paramagnetic

operator $h_t^{01,\mathrm{EPR}}$ of eq 28. The dia- and paramagnetic contributions to the *g*-shift are now

$$\Delta g^{\mathrm{d}}_{st} = \sum_{\gamma=\alpha,\beta} 2m_\gamma \sum_{i=1}^{n_\gamma} n_i^\gamma \times \left\{ \frac{g'}{4c^2} \left\langle \Psi_i \middle| \sum_{\nu}^{2M} \mathrm{d}_{\nu i} \left[\frac{\partial V_{\mathrm{eff}}}{\partial r} \cdot \vec{r}_\nu \delta_{st} - \left(\frac{\partial V_{\mathrm{eff}}}{\partial r} \right)_s r_{\nu_t} \right] \chi_\nu \right\rangle + \frac{1}{2c} \sum_{\lambda,\nu}^{2M} \mathrm{d}_{\lambda i} \mathrm{d}_{\nu i} \langle \chi_\lambda | [\vec{r}_\nu \times (\vec{R}_\nu - \vec{R}_\lambda)]_s h_t^{01,\mathrm{EPR}} | \chi_\nu \rangle \right\} \quad (34)$$

and

$$\Delta g^{\mathrm{p}}_{st} = \frac{1}{2c} \sum_{\gamma=\alpha,\beta} 2m_\gamma \sum_{i=1}^{n_\gamma} n_i^\gamma \sum_{\lambda,\nu}^{2M} \mathrm{d}_{\lambda i} \mathrm{d}_{\nu i} \times \langle \chi_\lambda | (\vec{R}_\lambda \times \vec{R}_\nu)_s h_t^{01,\mathrm{EPR}} | \chi_\nu \rangle + \Delta g^{\mathrm{p,oc-oc}}_{st} + \Delta g^{\mathrm{p,oc-vir}}_{st} \quad (35a)$$

where

$$\Delta g^{\mathrm{p,oc-oc}}_{st} = \sum_{\gamma=\alpha,\beta} 2m_\gamma \sum_{i,j=1}^{n_\gamma} n_i^\gamma S_{ij}^{1,s} \langle \Psi_i | h_t^{01,\mathrm{EPR}} | \Psi_j \rangle \quad (35b)$$

and

$$\Delta g^{\mathrm{p,oc-vir}}_{st} = 2 \sum_{\gamma=\alpha,\beta} 2m_\gamma \sum_{i=1}^{n_\gamma} n_i^\gamma \sum_{a}^{vir} u_{ai}^{1,s} \langle \Psi_i | h_t^{01,\mathrm{EPR}} | \Psi_a \rangle \quad (35c)$$

In eqs 34 and 35, we used the following notation: Ψ_i and Ψ_a are an occupied and virtual Kohn−Sham orbital,[51] respectively. The orbitals are expanded into the set of *2M* basis functions $\{\chi_\lambda\}$; the expansion coefficients are the $d_{\lambda i}$. The orbital Ψ_i has the occupation number n_i^γ; equal occupation numbers for all n_γ occupied orbitals of spin γ are assumed in the derivation of eq 35b.[64] Note that we used in eqs 34 and 35a the inverse of the speed of light *c* instead of the fine structure constant to avoid confusion with the α spin component (cf. ref 50). The definitions of the first-order occupied−occupied and occupied−virtual coefficients $S_{ij}^{1,s}$ and $u_{ai}^{1,s}$, respectively, are the same as those in the case of the NMR shielding, cf. our earlier work.[28−31] Finally, the coefficients $2m_\gamma$ in eqs 34 and 35 afford the correct signs for the α and β spins, in accordance with the spin-field reduction procedure of eq 22. Thus

$$m_\alpha = \frac{1}{2}$$

$$m_\beta = -\frac{1}{2} \quad (36)$$

The only contribution to Δg_{st} that does not follow from the EPR−NMR analogy (eq 32) is $\Delta g_{st}^{\mathrm{KE}}$. As has been pointed out before, it is due to the Zeeman kinetic energy correction, eq 29c. The operator in eq 29c is isotropic. Its contribution to $\Delta\vec{\vec{g}}$ is readily calculated from the ground state, zero-order density matrices (eqs 23 and 26, respectively) as

$$\Delta g_{st}^{\mathrm{KE}} = \delta_{st} \int_{\vec{r}\to\vec{r}'} \mathrm{d}\tau \; h_{st}^{11,\mathrm{KE}}(\vec{r}') [\rho^\alpha(\vec{r},\vec{r}') - \rho^\beta(\vec{r},\vec{r}')] \quad (37)$$

Details of the NMR−GIAO implementation into the Amsterdam Density Functional program package ADF[65−76] have been given elsewhere.[28−31] We employ the nonlocal exchange−correlation energy functionals that were developed by Becke and Perdew[77−80] for the self-consistent determination of the unperturbed electronic density.

We use Slater type orbitals (STO) as basis functions.[75,76] The STO basis sets are of triple-ζ quality in the valence region, unless otherwise stated. These triple-ζ basis sets are augmented by two sets of d-type polarization functions per atomic center (p polarization functions on hydrogen). The working equations for the *g*-shift, eqs 34, 35, and 37, are readily extended to include the frozen core approximation,[65,67] again in analogy to the NMR shielding tensor.[29,31] The frozen core approximation is a scheme in which only valence electrons are treated by the variational procedure. Molecular orbitals describing inner shells are precalculated; they are obtained from atomic calculations. These orbitals are kept "frozen" in subsequent molecular calculations. Hence, the frozen core approximation amounts to the neglect of core polarization. The valence molecular orbitals are explicitely orthogonalized aginst the (frozen) core orbitals. The frozen core approximation is employed throughout,[29,31] unless otherwise stated.

4. Results and Discussion

In this section, we will apply the formalism that has been developed thus far to actual *g*-tensor calculations. We will express the calculated and experimental numbers using the *g*-shift Δ*g* of eq 16. Our results will be compared to experiment[3,6,8,12,81−84] and to other, *ab initio* based calculations.[12−22] We have transferred all experimental numbers to *g*-shifts according to eq 16. They have been rounded to the nearest decimal according to the number of digits in the experimental *g*-tensor.

4.1. Geometries. EPR is concerned with systems containing unpaired electrons. Most of these systems are radicals that are usually not stable. Experimental geometries are therefore rare.[12,85,86] For this reason, we have based all of the calculations on optimized geometries. We used the ADF program for the optimization,[69,87−89] in part with its relativistic extension.[90] The results of these optimizations are summarized in the Supporting Information.

The EPR calculations were generally based on the relativistic geometry for such molecules where both nonrelativistic and relativistic results are given in the supplementary material. We note in passing the relativistic bond contraction.[42,90−94] For instance, the relativistic contraction of the l_{C-X} bond length in CF_3X^-, X = Cl, Br, or I, grows from an almost negligible 0.003 Å for X=Cl to 0.049 Å (about 2% of the bond length) for the iodine compound.

The following axis system was used: The *z* axis was always chosen to coincide with the axis of highest symmetry. Planar molecules are placed in the *yz* plane.

4.2. Comparison to Other Calculations. We shall next consider some *g*-shifts that were calculated with the previously developed formalism. We have pointed out in the introduction that *ab initio* calculations are surprisingly scarce. These calculations have been reviewed by Lushington,[12] and Lushington *et al.*[12,19−22] added their own significant contribution. We compare in Table 1 our DFT−GIAO results to the results of Lushington *et al.*[12,19−22] as well as to other *ab initio* calculations[13−18] and to experiment.[3,6,12,81−84] Lushington *et al.*[12,19−22] present results at various levels of sophistication. We included in Table 1 their "complete-to-second-order" HF results and the correlated MRCI calculations. We did not include the simpler calculations where only one-electron terms, *i.e.*, the operators $h_{\mathrm{SO-N}}$ and $h_{\mathrm{SO-N}}^{\mathrm{dia}}$ of eqs 4 and 7, respectively, have been accounted for.

TABLE 1: Calculated DFT−GIAO *g*-Shifts in comparison to *ab initio* and Experimental Results

		g-shifts Δ*g*(ppm)					
		calcd				exptl[c]	
molecule	component	DFT−GIAO[a]	HF	HF[b]	MRCI[b]	gas phase	other
H_2^+	$\Delta g_\perp$	−41.7	−2.25[d] −43.4[e]				
	$\Delta g_\parallel$	−39.3	−39.6[e]				
H_2O^+	Δg^{xx}	103		−324	−292	200	
	Δg^{yy}	13 824		16 361	16 019	18 800	
	Δg^{zz}	5126		4402	4217	4800	
CO^+	$\Delta g_\perp$	−3129		−1175	−2674	−2400	−2800[f] −2600[f] −3200[g]
	$\Delta g_\parallel$	−138		−176	−178		−1200[f] −1800[f] −1400[g]
CO_2^-	Δg^{xx}	1522	1800[h]				880[i] 600
	Δg^{yy}	−7210	−3900				−5070[i] −4900
	Δg^{zz}	−803	100				−710[i] −1100
O_3^-	Δg^{xx}	−554	0[k]				1300
	Δg^{yy}	19 380	28 940				16 400
	Δg^{zz}	10 542	11540				10 000
HCO	Δg^{xx}	2749	1800[h]				1500
	Δg^{yy}	−270	100				0
	Δg^{zz}	−9468	−5500				−7500
H_2CO^+	Δg^{xx}	6231	6500[h]				4600
	Δg^{yy}	−1220	400				−800
	Δg^{zz}	76	5600				200
C_3H_5	Δg^{xx}	−115	0[h]				0[l]
	Δg^{yy}	769	1000				400
	Δg^{zz}	660	800				800
NO_2^{2-}	Δg^{xx}	−472	0[k]				600[c] 1500[i]
	Δg^{yy}	9082	10010				5500[c] 7600[i]
	Δg^{zz}	4319	6970				4800[c] 4700[i]
NO_2	Δg^{xx}	4158	3460[m] 4700[h]	2257	3806	3900	3800[c] 3200[i] 3300[g]
	Δg^{yy}	−13 717	−10 274[m] −11 900[h]	−6597	−10322	−11300	−11700[c] −9100[i] −10 300[g]
	Δg^{zz}	−760	−218[m] 400[h]	−474	−235	−300	500[c] −2700[i] 700[g]
NF_2	Δg^{xx}	−738	0[k]				−100
	Δg^{yy}	7619	10180				6200
	Δg^{zz}	4678	4000				2800
NF_3^+	$\Delta g_\perp$	8046	4000[h]				7000
	$\Delta g_\parallel$	−511	400				1000
CN	$\Delta g_\perp$	−2514	−789[m]				−2000
	$\Delta g_\parallel$	−137					
MgF	$\Delta g_\perp$	−2178		−658	−1092		−1300
	$\Delta g_\parallel$	−60		−54	−59		−300

[a] This work. [b] G. Lushington *et al.*[12,19,20,22] [c] Cited from G. Lushington,[12] unless otherwise stated. All experimental values have been rounded to the nearest decimal. [d] Reference 13. [e] Reference 14. [f] Experimental cited from ref 82, solid neon matrix. [g] Neon matrix isolation experiment, cited from G. Lushington.[12] [h] Reference 15. [i] Experimental cited from ref 16. The solid matrices are $CaCO_3$ (CO_2^-), $NaNO_3$ (NO_2), and KCl (NO_2^{2-}). [k] Reference 16. [l] Argon matrix. The experimental principal axis orientation is not entirely clear from ref 84. [m] Reference 17.

It follows from Table 1 that our DFT−GIAO results are of better quality than any of the older HF calculations.[13−18] Lushington[12] has discussed these calculations. He points out that none of them include all the relevant operators. Further, most of these calculations are hampered by the use of very small basis sets. It is well-known that other magnetic properties require extended basis sets, even more so when no gauge-invariant scheme like GIAO or IGLO[95−98] is used.[35−37,99] We will come back to the basis set requirements later. The only cases where other calculations achieve better agreement with experiment then the DFT−GIAO method are NO_2[17] and possibly C_3H_5,[15] Table 1. However, Lushington[12] points out that the

excellent agreement between the calculations of Moores and McWeeny (for NO_2) and experiment is due to a cancellation of errors.

The H_2^+ radical is an interesting case. This is an one-electron system, and HF should be exact. The older one of the cited HF calculations[13] includes only the electron-nuclear spin−orbit operators, cf. eqs 4 and 7. The authors of the other article[14] included all the relevant operators, Table 1. It should be pointed out that the remaining differences between the HF results on the one hand and the DFT results on the other hand are minor as compared to the experimental accuracy. We cite all numbers in ppm. However, less significant digits are availabable from experiment, usually two or three digits less, and a change of ±50−100 ppm can be considered as small.

Let us now discuss our results in comparison to the complete-to-second-order HF and MRCI calculations of Lushington *et al.*[12,19−22] We can make this comparison for H_2O^+, CO^+, NO_2, and MgF, Table 1. A larger range of molecules would be desirable for a more comprehensive discussion. Gas phase data are available for the first three molecules. The DFT−GIAO calculations are in better agreement with experiment than the HF calculations for these molecules; the best results are obtained by the expensive MRCI calculations, Table 1. Similar trends have been observed in NMR shielding calculations.[100] All theoretical methods seem to have problems predicting the sign of very small contributions. Thus, we calculate the correct sign for the small xx principal component Δg^{xx} of H_2O^+ while the MRCI calculations have the wrong sign. Other cases are the parallel *g*-shift components $\Delta g_{||}$ of CO^+ and MgF. No gas phase data exist for these parallel components, and none of the theoretical methods reproduces the experimental order of magnitude for $\Delta g_{||}$ of CO^+. The parallel component of a diatomic molecule like CO^+ and MgF will have no contributions from the paramagnetic operators in our formulation, due to symmetry. This component is entirely determined by the diamagnetic contributions. The kinetic energy correction (eq 37) yields negative *g*-shifts. The other contributions should be positive since they contain essentially only an integral over the density of the singly occupied molecular orbital (SOMO) multiplied with a positive function (eqs 19 and 34). We speculate that large negative experimental values for the parallel component of linear molecules might be due to matrix effects.

Correlation effects, as evident from the difference between HF and MRCI calculations, can be considerable for *g*-shifts and their tensor components, Table 1. They are comparatively small in saturated systems with single bonds (like H_2O^+) that usually have large HOMO−LUMO gaps. This agrees with the situation for the NMR shielding, again demonstrating the close connection between the two properties.[28,31] In other molecules like CO^+, NO_2, or MgF, there is a considerable difference between the results that were calculated at the HF level and at the MRCI level, respectively. Correlation is necessary for a proper description of these molecules. The influence of electron correlation is expected to be most prominent in the paramagnetic contributions that contain the first-order magnetic wave function, section 2. This is indeed the case, as is evident from the parallel component of the *g*-shift in the linear molecules CO^+ and MgF, Table 1. As has been pointed out before, the parallel component in linear molecules does not contain the first-order magnetic orbitals. It is exclusively diamagnetic, containing the unperturbed, zero-order density matrix. The remaining changes in these molecules, 2 ppm for CO^+, and −5 ppm for MgF, Table 1, can be attributed to slight changes in the electron density of the SOMO that are due to the introduction of correlation.

TABLE 2: Calculated and Experimental *g*-Shifts of Diatomic Molecules (Values in ppm)

	$\Delta g_{\|\|}$		$\Delta g_{\perp}$	
molecule	calcd	exptl	calcd	exptl
CO^+	−138	−1200[a]	−3129	−2800[a]
		−1800[a]		−2600[a]
		−1400[b,c]		−3200[b,c]
				−2400[c,d]
CN	−137	−800[e]	−2514	−2000[e]
AlO	−142	−800[e]	−222	−1900[e]
		−900[e]		−2600[e]
		−3000[e]		−8600[e]
BO	−72	−1100[e]	−2298	−800[e]
BS	−83	−700[e]	−9974	−8100[e]
		−800[e]		−7900[e]
MgF	−60	−300[b,c]	−2178	−1300[b,c]
KrF[f]	−335 (−345)	−2000[g]	60 578 (61 851)	66 000[g]
XeF[f]	−340 (−346)	−28 000[g]	15 1518 (158 083)	12 4000[g]

[a] Experimental cited from ref 82, solid neon matrix. [b] Neon matrix isolation experiment. [c] Cited from ref 12. [d] Gas phase experiment. [e] Cited from ref 6. The different values correspond to different matrices (in this order: CN, argon matrix; AlO, neon, argon, and krypton matrix; BO, neon matrix; BS, neon and argon matrix). [f] Calculation based on nonrelativistic and (in brackets) scalar relativistic wave function. [g] Radicals embedded in KrF_4 and XeF_4 crystals, respectively (cited from ref 81).

4.3. Diatomic Radicals. In Table 2, we have collected results for some diatomic radicals. Two of them, CO^+ and MgF, have been discussed in the previous section.

We see from Table 2 that the DFT−GIAO method is unable to reproduce the parallel component of the *g*-shift $\Delta g_{||}$ in cases where this component has a large negative value. We have discussed the point above, speculating that these negative values might be due to matrix effects.

The range of experimental numbers can be considerable, cf., *e.g.*, the data for CO^+ or AlO, Table 2. Nevertheless, almost all experimental trends are reproduced by the DFT−GIAO method. Gas phase experiments are available for the orthogonal components of CO^+, CN, and MgF. We obtain good agreement for CO^+ and CN, and reasonable agreement for MgF.

All three sets of solid state data for CO^+ (Tables 1 and 2) refer to neon matrices. This should be a very inert solvent system. Nevertheless, the three sets of data do not agree with each other, nor do they match the available gas phase value for the orthogonal principal *g*-shift component of this compound, Tables 1 and 2. The example illustrates the importance and magnitude of matrix effects.

The worst case of the diatomic molecules in Table 2 is the AlO radical. We miss in this case the experimental trend completely, even though the experimental numbers differ considerably, depending on the matrix. The reason for this apparent failure of the current theoretical method is not entirely clear at the moment; we will come back to this point later on.

The two noble gas fluorides KrF and XeF have been treated with the scalar relativistic procedure that had been developed for shielding calculations.[30,31] We see from Table 2 that relativistic effects are unimportant for the diamagnetic parallel component of the *g*-shift. The change in this component would mostly reflect changes in the electronic density of the SOMO; these effects are expected to be not very big.[42,91] Larger scalar relativistic effects are observed in the paramagnetic orthogonal component, in particular for XeF.

4.4. G-Shifts of AB_3, AB_2, and Other Radicals. Calculated and experimental *g*-shifts for several AB_3 radicals have been collected in Table 3. These molecules possess a 3-fold

TABLE 3: Calculated and Experimental *g*-Shifts of AB_3 Molecules (Values in ppm)

	isotropic Δg		$\Delta g_{\|\|}$		$\Delta g_{\perp}$	
molecule	calcd	exptl	calcd	exptl	calcd	exptl
CO_3^-	8934	8900[a]	3361	4300[a]	11 810	11 200[a,b]
NO_3	8009	10500[a]	47	4300[a]	11 969	13 550[a,b]
NO_3^{2-}	3208	2000[a,c]	−563	−800[a,c]	5094	3400[a,c]
NH_3^+	1319	1200[d]	−146		2051	
		900[e]				
NF_3^+	5193	5000[f]	−511	1000[f]	8046	7000[f]
PO_3^{2-}	−767	−2000[g]	−415	−3000[g]	−944	−1000[g]
		−2000[a]		−2900[a]		−1550[a,b]
SO_3^-	1641	1300[g]	301		2311	
ClO_3	4644	6000[a]	1575	5000[a]	6179	6000[a]
		8700[g]		4300[g]		10 900[g]
AsO_3^{2-}	−4757	3000[a]	−569	2000[a]	−6951	3000[a]
CH_3	470	−300 to 340[h]	−91		750	
SiH_3	1566	4000[i]	−105	1000[i]	2402	5000[i]
GeH_3	12 756	10 000[i]	30	1000[i]	19 119	15 000[i]
SnH_3	28 562[k]	15 000[i]	312[k]	1000[i]	42 688[k]	23 000[i]

[a] Cited from ref 81. Solid matrices: $KHCO_3$ for CO_3^-, urea nitrate for NO_3, $Na_2HPO_3 \cdot 5H_2O$ for PO_3^{2-}, NH_4Cl_4 for ClO_3, $Na_2HAsO_4 \cdot 7H_2O$ for AsO_3^{2-}. [b] Average of the two orthogonal principal components (measured as 16 100 and 6300 for CO_3^-, 18 000 and 9100 for NO_3; −1200 and −1900 ppm for PO_3^{2-}). [c] See Table 4 for other experimental values.[83] [d] Cited from ref 6. [e] Cited from ref 82. [f] Cited from ref 12. [g] Cited from ref 3. Solid matrices: $Na_2HPO_3 \cdot 5H_2O$ for PO_3^{2-}, $K_2CH_2(SO_3)_2$ for SO_3^-, $KClO_4$ for ClO_3. [h] The following isotropic experimental *g*-shifts were found at 4.2 K:[6] −290 ppm (Ar matrix), −300 ppm (Xe matrix), 340 ppm (H_2 matrix), −290 ppm (N_2 matrix), 100 ppm (CH_4 matrix). The anisotropy of the *g*-shift is too small to be measured. [i] Derived values for static radicals, the radicals are thought to undergo restricted rotation—even at 4.2 K.[6] [k] Calculated with a scalar relativistic wave function.

TABLE 4: Experimental *g*-Shifts of the NO_3^{2-} Radical in Different Host Crystals

	principal components of Δg(ppm)[a]			
host matrix	isotropic	Δg^{xx}	Δg^{yy}	Δg^{zz} [b]
KNO_3	2000	3400		−800
$Sr(NO_3)_2$	2300	3700		−400
$Ba(NO_3)_2$	1400	3400		−2600
$NaNO_3$	1500	2900		−1200
KCl	2900	4500		−300
KBr	2900	4500		−300
KI		2700		
KN_3	100	1600		−2900
$Pb(NO_3)_2$	−12 900	−11 100		−16 600
$AgNO_3$	700	−300	4700	−2300
calcd[c]	3208	5094		−563

[a] Cited from ref 83. [b] The *z* axis is orthogonal to the O_3 plane. [c] This work.

symmetry axis. The principal tensor components of the *g*-shift correspond to coordinate axes that are parallel ($\Delta g_{||}$) and orthogonal ($\Delta g_{\perp}$) to this symmetry axis. One of these molecules, NF_3^+, has already been discussed above, Table 1.

The experimental numbers were generally obtained with the radical embedded in some host crystal. This makes the comparison of calculated and experimental numbers difficult since the calculations refer to the zero-pressure and zero-temperature limit of a gas phase experiment. Experimental values can, on the other hand, vary considerably with the host crystal. An example[6] of this has been given in Table 3 for the isotropic *g*-shift of CH_3; another example[83] is given in Table 4 for NO_3^{2-}. We see from Table 4 and Figure 1 that the experimental range is enormous, making the comparison with the calculated results very difficult if not impossible. The calculated numbers exhibit at least the right trend with the orthogonal *g*-shift being much larger then the parallel component. The calculated anisotropy, *i.e.*, the difference between

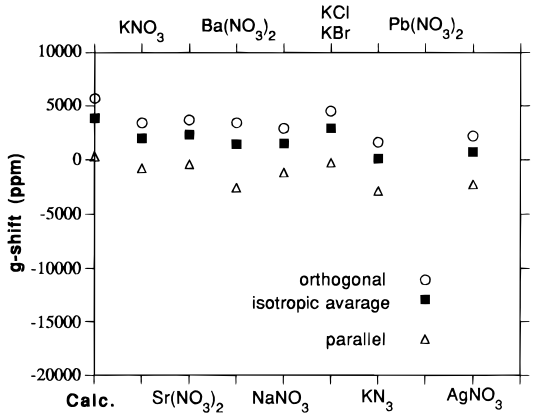

Figure 1. Experimental *g*-shifts of the NO_3^{2-} radical in different host crystals.

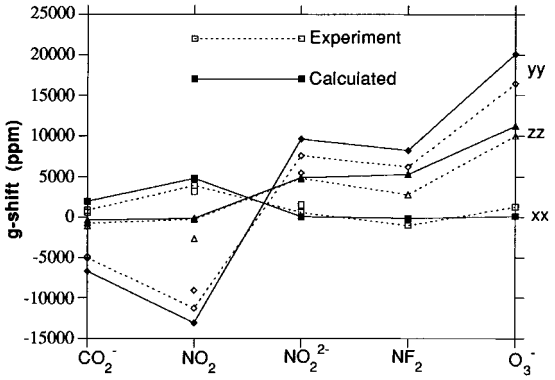

Figure 2. Principal tensor components of the *g*-shift in symmetric AB_2 radicals of first-row compounds.

parallel and orthogonal principal components, has the correct sign and the right order of magnitude.

Given this uncertainty in the comparison of theory and experiment, we note from Table 3 that the agreement between theory and experiment is reasonable to good in most cases. Experimental trends within related compounds are mostly reproduced (*e.g.*, in the series PO_3^{2-}, SO_3^-, and ClO_3). One of these trends is the increase in the isotropic *g*-shift and its tensor components when going down within a column of the periodic table of elements; the example here is the series of compounds EH_3, E = C, Si, Ge, or Sn. The trend is reproduced by the calculations. The calculated *g*-shifts of GeH_3 and in particular SnH_3 are, however, too big. The same is the case for other heavy element compounds: the calculated *g*-shift of AsO_3^{2-} does not match the experimental results. We will come back to this point shortly.

It is also interesting to look at the *g*-shifts of symmetric AB_2 radicals. Several of them, namely H_2O^+, CO_2^-, O_3^-, NO_2, NO_2^{2-}, and NF_2 have been included already into Table 1. The data for most of these radicals is also contained in Figure 2. We note again the considerable range of experimental single-crystal results as exemplified for these compounds by NO_2, Table 1. The results are essentially similar to the AB_3 case. Thus, experimental trends, both regarding the principal tensor components and trends between related molecules, are reproduced for these first-row compounds, Figure 2. Two more AB_2 radicals, ClO_2 and SO_2^- are contained in Table 5. We have included the latter two to get a more comprehensive picture. The agreement between theory and experiment is reasonable but not perfect for these two molecules. Part of this are probably again matrix effects.

A few other compounds have been included into Table 5. This was done to cover some other classes of compounds as

TABLE 5: Calculated and Experimental *g*-Shifts of Some Other Molecules

	principal components of Δg(ppm)					
	Δg^{xx}		Δg^{yy}		Δg^{zz}	
molecule	calcd	exptl	calcd	exptl	calcd	exptl
ClO_2	−455	1300[a]	12 292	16 000[a]	10 606	6500[a]
SO_2^-	−361	−400[a]	5588	9700[a]	7178	3400[a]
CH_4^+	−48	600[b]	−48	600[b]	−48	600[b]
benzene$^+$ [c]	445		445		11	

[a] Experimental cited from ref 6; $KClO_4$ host crystal for ClO_2, $K_2S_2O_5$ for SO_2^-. [b] Experimental cited from ref 82. [c] Isotropic *g*-shift: 300 ppm, calcd; 400 ppm, exptl.[82]

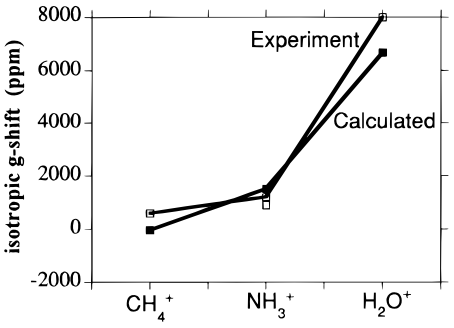

Figure 3. Isotropic *g*-shifts in CH_4^+, NH_3^+, and H_2O.

TABLE 6: Calculated and Experimental *g*-Shifts of CF_3X^-, X = Cl, Br, or I (Values in ppm)

	$\Delta g_{\|\|}$			$\Delta g_\perp$		
	calcd			calcd		
molecule	non-relativistic	relativistic	exptl[a]	non-relativistic	relativistic	exptl[a]
CF_3Cl^-	−609	−610	−200	14 873	15 112	4 700
CF_3Br^-	−635	−637	1 300	67 273	70 229	18 900
CF_3I^-	−581	−571	−2 100	146 759	161 466	46 000

[a] Cited from ref 6.

well. Thus, CH_4^+, together with NH_3^+, Table 3, and H_2O^+, Table 1, comprise three hydride cations of first-row compounds, Figure 3. The experimental isotropic *g*-shifts are 600, 1200/900, and 8000 ppm for CH_4^+, NH_3^+, and H_2O^+, respectively. The calculated numbers are −48, 1319, and 6035 ppm. The periodic trend within this group is therefore well reproduced by the calculations, Figure 3. We have also included the benzene cation into Table 5. This is an example for an aromatic radical; again, the isotropic *g*-shift is well reproduced.

To conclude this section, we collected in Table 6 calculated and experimental *g*-shifts for the anionic radicals CF_3X^-, X = Cl, Br, or I. This turns out to be a case where the current theoretical method is apparently unable to reproduce the experimentally observed trend. We will discuss this point in the conclusions.

4.5. Contributions to the *g*-shifts. The relative importance of the various contributions in the theoretical description of the *g*-shifts might be of interest. For this purpose, we have split the calculated *g*-shifts of CO^+ and H_2O^+ into their contributions. The results are summarized in Tables 7 (CO^+) and 8 (H_2O^+). The total *g*-shift is initially split into contributions due to the dia- and paramagnetic operators, eqs 7−9 and 4−6, respectively, as well as the isotropic contribution from the kinetic energy correction, eqs 3 and 37. The kinetic energy correction is always negative. It yields a small but significant contribution to the *g*-shift, Tables 7 and 8. The paramagnetic contributions are dominant, both for the isotropic *g*-shift and for the individual tensor components. The diamagnetic (or gauge correction[4])

TABLE 7: Contributions to the Calculated *g*-Shift of CO^+ (Values in ppm)

	tensor components		
contribution	isotropic	parallel	orthogonal
total	−2123	−135	−3117
total diamagnetic	53	46	57
total paramagnetic	−1995	0	−2993
kinetic energy correction	−181	−181	−181
nuclear potential			
total contribution	−2346	81	−3559
diamagnetic	106	81	119
paramagnetic	−2452	0	−3678
Coulomb potential (electronic density)			
total contribution	513	−43	791
diamagnetic	−61	−43	−69
paramagnetic	574	0	860
Exchange potential			
total contribution	−109	9	−168
diamagnetic	8	9	8
paramagnetic	−117	0	−176

TABLE 8: Contributions to the Calculated *g*-Shift of H_2O^+ (Values in ppm)

	tensor components			
contribution	isotropic	xx	yy	zz
total	6016	−209	13 457	4800
total diamagnetic	120	92	124	145
total paramagnetic	6206	9	13 644	4965
kinetic energy correction	−310	−310	−310	−310
nuclear potential				
total contribution	7859	147	17 024	6407
diamagnetic	206	147	216	254
paramagnetic	7653	0	16 808	6153
Coulombic potential (electronic density)				
total contribution	−1931	−58	−4109	−1625
diamagnetic	−99	−68	−105	−123
paramagnetic	−1832	10	−4004	−1502
exchange potential				
total contribution	398	13	852	328
diamagnetic	13	14	13	14
paramagnetic	284	−1	839	314

contribution is much smaller then its paramagnetic counterpart. It is, however, not negligible in most cases.

In Tables 7 and 8, we have also further split up the *g*-shifts. This has been done according to the different contributions to the effective potential of eq 21. The nuclear potential, V_N, eq 13, is the largest contribution in all cases. Using only V_N would amount to the exclusive use of the one-electron operators, eqs 4 and 7. It is clear from Tables 7 and 8 that the two-electron operators have to be included for an accurate description of the *g*-shift. The two-electron operators are represented as the contributions from the Coulomb potential V_C of the electronic density, eq 20, and the exchange potential, $V_{X\alpha}$. Their contributions are generally smaller then the *g*-shifts due to V_N. Nevertheless, these contributions are not negligible.

Finally, we note from Tables 7 and 8 that the exchange potential gives the smallest *g*-shift contributions. This justifies the use of the simple X_α approximation[61] for this part: even if the relative error in this contribution was large, it would still not really change the total calculated *g*-shifts.

4.6. Basis Sets. All calculated results so far have been obtained by using just one basis set. It remains to show that our standard basis set is saturated to a reasonable degree: That is the subject of this section.

The basis set dependence of calculated NMR chemical shifts is well-known.[36,37,98,99,101] From the analogy of the EPR *g*-tensor and the NMR shielding, we would expect a similarly strong basis set dependence for the *g*-tensor. The basis set dependence

TABLE 9: Calculated *g*-Shifts for Various Basis Sets (Values in ppm)

	basis						
molecule	III[a]	IV[a]	V[a]	td[a]	td[b]	tf[a]	qd[c]
CH_3	460	472	476	469	470	475	502
CH_4^+	−36	−51	−51	−50	−50	−52	−56
NH_3^+	1239	1295	1314	1320	1323	1330	1390
H_2O^+	5506	5998	6000	6031	6035	6006	6214
HCO	−2080	−2372	−2349	−2329	−2329	−2312	−2320
H_2CO^+	1569	1702	1696	1693	1696	1697	1751
CO^+	−1953	−2133	−2128	−2128	−2132	−2129	−2182
CN	−1540	−1720	−1707	−1720	−1721	−1711	−1752
CO_3^-	7840	9058	9016	8990	8994	8942	9138
NO_3	7103	8046	8039	8004	8009	8020	8266
NO_3^{2-}	3044	3265	3256	3211	3208	3199	3197
NF_2	3527	3843	3825	3822	3853	3836	3950
NF_3^+	4577	5194	5161	5161	5193	5163	5320

[a] Single-ζ core. [b] Double-ζ core. [c] All-electron basis.

TABLE 10: Basis Sets

basis	explanation
III	standard basis set of ADF:[a] double-ζ valence region; one set of d polarization functions (p on hydrogen)
IV	standard basis set of ADF:[a] triple-ζ valence region; one set of d polarization functions (p on hydrogen)
V	standard basis set of ADF:[a] same as IV but additionally one set of f polarization functions (d on hydrogen)
td	same as IV but two sets of d (p) polarization functions; single- or double-ζ core region of the basis
tf	same as td but additionally one set of f polarization functions (d on hydrogen)
qd[b]	all-electron basis, triple-ζ in the core, quadruple-ζ in the valence region, two sets each of d and f polarization functions (p and d on hydrogen)

[a] ref 69,75,76. [b] ref 102.

of calculated *g*-shifts has been addressed in Table 9. This table contains calculated isotropic *g*-shifts for several molecules containing hydrogen, carbon, nitrogen, oxygen, or fluorine atoms. We employed double-ζ (basis III), triple-ζ (IV, V, td, tf)[69,75,76] and quadruple-ζ (qd)[102] valence basis sets. All basis functions are Slater type orbitals (STO). Details of the different basis sets have been summarized in Table 10.

Several conclusions can be drawn from Table 9. First, it should be noted that we cite all numbers in ppm. In general, less signifcant digits are available from experiment, cf. Tables 1 to 6. This has been pointed out above already. Thus, a change of ±100 ppm or less in calculated numbers between two basis sets can be considered as essentially converged. With this in mind, we note that the double-ζ basis is not sufficient; the various triple-ζ sets give much more consistent results. The largest deviations between the previously employed td set and the more accurate qd basis amount to 262 ppm for NO_2, followed by 183, 159, and 148, and 128 ppm for H_2O^+, NF_3^+, CO_3^-, and NF_2, respectively (Table 9). Consequently, the td basis is not yet completely saturated for these molecules and the more accurate qd basis would be preferable in these cases. However, the remaining basis set error is small as compared to the deviation between theory and experiment, Tables 1 and 3, or as compared to matrix effects, Table 4. We can infer that the td basis was indeed sufficient to test the present method and to draw meaningful conclusions from the calculated *g*-shifts.

Additionally, it follows from Table 9 that the 1s (core type) basis functions are of only minor importance for the calculation of *g*-shifts. In the case of the "tight" NMR shielding, more care had to be taken in defining the core region of the basis sets. This was necessary to describe the core tail of valence orbitals correctly.[29,30,100] The *g*-shift, on the other hand, is less "tight", and the difference between the basis sets with single- and double-ζ cores is only marginal, Table 9. More important than the core region is a sufficient number of polarization functions in the basis sets. Basis sets IV, V, td, and tf are all triple-ζ valence basis sets with various combinations of d- and f-type polarization functions. The d and f sets seem to be of different importance in different classes molecules. The addition of a second set of d functions has almost no influence in some cases like CH_3 or CN (as evident by comparing the results of IV and td, or V and tf), but is important in other cases like CO_3^-, NO_3, or NO_3^{2-}. Similarly, the additional f set in basis sets V and tf changes the results for some molecules like HCO or CO_3^-, but is unimportant for others like CH_4^+ or NO_3. The differences between the various triple-ζ are in almost all cases smaller than 100 ppm.

Further studies of basis set requirements, also including heavier elements are desirable.

5. Summary and Conclusions

We presented in this paper a formulation of the EPR *g*-tensor and the EPR *g*-shift based on density functional theory. We have also implemented our formulation into the existing DFT−GIAO program system for NMR chemical shifts that has been described elswhere.[28−32] Our implementation is the only first-principle DFT method for the calculation of the *g*-tensor, even though the interest in this property seems to be growing recently.[102,103] Our method is also the first GIAO implementation of the *g*-tensor. Lushington discussed the gauge dependence of his results;[12] the gauge dependence is minimized by choosing the centroid of charge as the common gauge origin for the given molecule. In this way, the gauge dependence of the calculated results is found to be only moderate. Nevertheless, fairly big basis sets are still necessary, and the GIAO scheme is expected to converge much faster with the basis set size than Lushington's method.[104]

We have compared our calculated results with experiment and with the HF and MRCI calculations of Lushington *et al.*[12,19−22] Comparison with experimental results is preferably done based on the (rare) gas phase data. We find that our method yields results of higher quality then the Hartree−Fock-based schemes. The highly expensive MRCI method gives the best results for the few molecules where a comparison is possible. This is in line with the situation for the NMR chemical shift,[100] stressing the close connection between the two magnetic properties.

The comparison to experimental data is more complex if that data has been obtained with the radical situated in a host crystal, due to the sometimes strong interactions of the radical with its matrix. Nevertheless, experimental trends for various small first- and second-row radicals have been reproduced with satisfying accuracy. Our calculated results are generally less accurate for compounds of heavier elements—up to what must be called complete failure. Examples included AlO and XeF, Table 2, AsO_3^{2-}, Table 3, and the molecules in Table 6.

It is now the point to discuss possible reasons for these limitations of the method. To find and judge possible reasons, we have to recall the derivation of our DFT−GIAO formulation. In doing this, we note that we had neglected the spin−other-orbit operators of eqs 6 and 9. This could of course be a possible reason for the observed deviations. However, contributions of these operators are expected to be small for systems with just one unpaired electron, cf. the discussion above. Only systems with one unpaired electron have been considered, and we don't expect the spin−other-orbit operators to be of importance. This is also confirmed by the success of the model for lighter element compounds.

Another approximation is the use of the simple X_α scheme as the exchange contribution to the effective potential, eq 21. We expect the contribution of this term to be very small in general, as has been the case for selected molecules, Tables 7 and 8. The approximation is therefore not significant, and it is an unlikely candidate for the explanation of the problems. This is again confirmed by the success of the model for lighter elements.

It is, however, well possible that the exchange−correlation (XC) functional[78−80] that is used in the self-consistent solution of the Kohn−Sham equations is still insufficient. It is well-known that the currently used gradient-corrected XC functionals exhibit the wrong asymptotic behavior both in the region close to the nucleus and in the limit of the coordinate going to infinity.[105,106] The latter range is expected to influence the values of the Kohn−Sham orbital energies (eigenvalues). The first-order magnetic density matrix, eq 27, is, in turn, extremely sensitive to small changes in these eigenvalues.[28,31]

The *g*-tensor has been treated as a second-order property in our model, cf. eqs 1 and 27. However, the experimental *g*-tensors are in general obtained by fitting the observed resonance energies ΔE to the Zeeman energy expression with expressions like the following one.[3,9] We have, for instance, for systems with one unpaired electron:

$$\Delta E = \mu_B \vec{S} \cdot \vec{\vec{g}} \cdot \vec{B} \tag{38}$$

To simulate the experimental procedure of eq 38 requires the inclusion of the spin−orbit operators (*i.e.*, the perturbation due to the electronic spin) to all orders in the spin magnetic moment $\vec{S}$. Our formulation is, however, based on perturbation theory, and the spin−orbit operators are included only up to first order. This could be a reason for the mentioned failure of the method. Spin−orbit splitting is a relativistic effect. Effects of relativity are known to increase with increasing atomic numbers *Z*; they are roughly proportional to Z^2.[42] Thus, it is conceivable that perturbation theory becomes less and less accurate with growing atomic numbers. One would have to calculate the electronic density up to all orders in the spin−orbit splitting instead of up to first order in the magnetic field. We plan to address this point in the future in more detail.

There are also other interesting extensions possible or necessary to the work that was presented in this chapter. One of them concerns the range of compounds that were included. In this paper, we have mainly concentrated on first- and second-row main group radicals. Transition metal chemistry is another major field for EPR measurements, and we plan to extend our investigations to this area.

Acknowledgment. This work has been supported by the National Science and Engineering Research Council (NSERC) of Canada and in part by the donors of the Petroleum Research Fund, administered by the American Chemical Society (ACS-PRF Grant 31205-AC3). We are grateful to Erik van Lenthe for stimulating discussions and for providing his large basis sets. G.S. acknowledges the Graduate Faculty Council, University of Calgary, for a scholarship.

Supporting Information Available: Definition of geometry parameters (Figure 4) and optimized geometries of radicals (Tables 11−15) (6 pages). Ordering information is given on any current masthead page.

References and Notes

(1) Mason, J., Ed. *Multinuclear NMR*; Plenum Press: New York, 1987.
(2) NATO ASI Series C, Mathmetical and Physical Sciences, 386; *Nuclear Magnetic Shieldings and Molecular Structure*; Tossell, J. A., Ed. Kluwer Academic Publishers: Dordrecht, The Netherlands, 1993.
(3) Wertz, J. E.; Bolton, J. R. *Electron Spin Resonance*; Chapman and Hall: New York, London, 1986.
(4) Harriman, J. E. *Theoretical Foundations of Electron Spin Resonance*; Academic Press: New York, 1978.
(5) Symons, M. *Chemical and Biological Aspects of Electron Spin Resonance Spectroscopy*; John Wiley & Sons: New York, 1978.
(6) Gordy, W. *Theory and Applications of Electron Spin Resonance*; John Wiley & Sons: New York, 1980.
(7) Kaiser, E. T., Kevan, L., Ed. *Radical Ions*; John Wiley & Sons: New York, 1968.
(8) Al'tshuler, S. A.; Kozyrev, B. M. *Electron Paramagnetic Resonance in Compounds of Transition Elements*; John Wiley & Sons: New York, 1974.
(9) Abragam, A.; Bleaney, B. *Electron Paramagnetic Resonance of Transition Ions*; Clarendon Press: Oxford, 1970.
(10) Mabbs, F. E.; Collins, D. *Electron Paramagnetic Resonance of d Transition Metal Compounds*; Elsevier: Amsterdam, The Netherlands, 1992.
(11) Cremer, D.; Olsson, L.; Reichel, F.; Kraka, E. *Isr. J. Chem.* **1993**, *33*, 369.
(12) Lushington, G. H. Ph.D. Thesis, University of New Brunswick, Fredericton, New Brunswick, Canada, 1996.
(13) de Montgolfier, P.; Harriman, J. E. *J. Chem. Phys.* **1971**, *55*, 5262.
(14) Hegstrom, R. A. *Phys. Rev. A* **1979**, *19*, 17.
(15) Ishii, M.; Morihashi, K.; Kikuchi, O. *J. Mol. Struct.* **1991**, *325*, 39.
(16) Hayden, D. W.; McCain, D. C. *J. Chem. Phys.* **1972**, *57*, 171.
(17) Moores, W. H.; McWeeny, R. *Proc. R. Soc. London, Ser. A* **1973**, *332*, 365.
(18) Larsson, S.; Hehenberger, M.; Correa de Mello, P. *Int. J. Quantum Chem.* **1980**, *18*, 1271.
(19) Lushington, G. H.; Bündgen, P.; Grein, F. *Int. J. Quantum Chem.* **1995**, *55*, 377.
(20) Lushington, G. H.; Grein, F. *Theor. Chim. Acta* **1997**, in print.
(21) Lushington, G. H.; Bruna, P. J.; Grein, F. *Z. Phys. D* **1996**, *36*, 301.
(22) Lushington, G. H.; Grein, F. *Int. J. Quantum Chem.* **1996**, *60*, 467.
(23) London, F. *J. Phys. Radium* **1937**, *8*, 397.
(24) Ditchfield, R. *Mol. Phys.* **1974**, *27*, 789.
(25) Malkin, V. G.; Malkina, O. L.; Salahub, D. R. *Chem. Phys. Lett.* **1993**, *204*, 80.
(26) Malkin, V. G.; Malkina, O. L.; Salahub, D. R. *Chem. Phys. Lett.* **1993**, *204*, 87.
(27) Malkin, V. G.; Malkina, O. L.; Casida, M. E.; Salahub, D. R. *J. Am. Chem. Soc.* **1994**, *116*, 5898.
(28) Schreckenbach, G.; Ziegler, T. *J. Phys. Chem.* **1995**, *99*, 606.
(29) Schreckenbach, G.; Ziegler, T. *Int. J. Quantum Chem.* **1996**, *60*, 753.
(30) Schreckenbach, G.; Ziegler, T. *Int. J. Quantum Chem.* **1997**, *61*, 899.
(31) Schreckenbach, G. Ph.D. Thesis, University of Calgary, Calgary, Alberta, Canada, 1996.
(32) Schreckenbach, G.; Dickson, R. M.; Ruiz-Morales, Y.; Ziegler, T. In *Chemical Applications of Density Functional Theory;* ACS Symposium Series 629; Laird, B. B., Ross, R. B., Ziegler, T., Eds.; American Chemical Society: Washington, DC, 1996; p 328.
(33) Rauhut, G.; Pulay, P. *J. Phys. Chem.* **1996**, *100*, 6310.
(34) Cheeseman, J. R.; Trucks, G. W.; Keith, T. A.; Frisch, M. J. *J. Chem. Phys.* **1996**, *104*, 5497.
(35) Fukui, H. *Magn. Reson. Rev.* **1987**, *11*, 205.
(36) Chesnut, D. B. In *Annual Reports on NMR Spectroscopy;* Webb, G. A., Ed.; Academic Press: New York, 1989; Vol. 21.
(37) Chesnut, D. B. In *Annual Reports on NMR Spectroscopy*; Webb, G. A., Ed.; Academic Press: New York, 1994; Vol. 29.
(38) Ruiz-Morales, Y.; Schreckenbach, G.; Ziegler, T. *J. Phys. Chem.* **1996**, *100*, 3359.
(39) Ruiz-Morales, Y.; Schreckenbach, G.; Ziegler, T. *Organometallics* **1996**, *15*, 3920.
(40) Epstein, S. T. *The Variation Method in Quantum Chemistry*; Academic Press: New York, 1974.
(41) McWeeny, R. *Methods of Molecular Quantum Mechanics*, 2nd ed.; Academic Press: London, New York, 1989.
(42) Pyykkö, P. *Chem. Rev.* **1988**, *88*, 563.
(43) Dalgarno, A.; Steward, A. L. *Proc. R. Soc. London, Ser. A* **1956**, *238*, 269.
(44) Dalgarno, A.; Steward, A. L. *Proc. R. Soc. London, Ser. A* **1957**, *240*, 274.
(45) Dalgarno, A.; Steward, A. L. *Proc. R. Soc. London, Ser. A* **1958**, *247*, 245.
(46) Moss, R. E. *Advanced Molecular Quantum Mechanics*; Chapman and Hall: London, 1973.

(47) Malkin, V. G.; Malkina, O. L.; Erikson, L. A.; Salahub, D. R. In *Modern Density Functional Theory: A Tool for Chemistry*; Politzer, P., Seminario, J. M., Eds.; Elsevier: Amsterdam, The Netherlands, 1995; Vol. 2, p 273.
(48) Atkins, P. W. *Physical Chemistry*, 5th ed.; Freeman: New York, 1995.
(49) Landau, L. D.; Lifshitz, E. M. *Quantum Mechanics (Non-Relativistic Theory)*; Pergamon Press: Oxford, New York, 1977.
(50) Equation 12 is in the given form only correct in atomic units where $1/c = \alpha$. More precisely, one would have to put $1/c$ as the prefactor of the vector potential in eq 12 and in all equations that are based on this substitution.
(51) Parr, R. G.; Yang, W. *Density-Functional Theory of Atoms and Molecules*; Oxford University Press: New York, Oxford, 1989.
(52) Ziegler, T. *Chem. Rev.* **1991**, *91*, 651.
(53) Ziegler, T. *Can. J. Chem.* **1995**, *73*, 743.
(54) Labanowski, J. K., Andzelm, J. W., Eds. *Density Functional Methods in Chemistry*; Springer-Verlag: Berlin, New York, 1991.
(55) Politzer, P., Seminario, J. M., Eds. *Modern Density Functional Theory: A Tool for Chemistry*; Elsevier: Amsterdam, The Netherlands, 1995.
(56) *Chemical Applications of Density Functional Theory*; ACS Symposium Series 629; Laird, B. B., Ross, R. B., Ziegler, T., Eds.; American Chemical Society: Washington, DC, 1996.
(57) The implementation of the gradient of this potential is partly due to D. Swerhone, A. Bérces, and H. Jacobsen (D. Swerhone, private communication, Calgary, 1996).[58−60]
(58) Bérces, A. Ph.D. Thesis, University of Calgary, Calgary, Alberta, Canada, 1995.
(59) Bérces, A.; Dickson, R. M.; Fan, L.; Jacobsen, H.; Swerhone, D.; Ziegler, T. *Comput. Phys. Commun.* **1997**, in print.
(60) Jacobsen, H. Ph.D. Thesis, University of Calgary, Calgary, Alberta, Canada, 1995.
(61) Slater, J. C. *Phys. Rev. A* **1951**, *81*, 385.
(62) Hohenberg, P.; Kohn, W. *Phys. Rev. B* **1964**, *136*, 864.
(63) Kohn, W.; Sham, L. J. *Phys. Rev. A* **1965**, *140*, 1133.
(64) It is possible to drop this condition, resulting in a modified version of eq 35b.[31]
(65) Baerends, E. J.; Ellis, D. E.; Ros, P. *Chem. Phys.* **1973**, *2*, 41.
(66) Baerends, E. J.; Ros, P. *Chem. Phys.* **1973**, *2*, 52.
(67) Baerends, E. J. Ph.D. Thesis, Free University, Amsterdam, The Netherlands, 1973.
(68) Baerends, E. J.; Ros, P. *Int. J. Quantum Chem., Quantum Chem. Symp.* **1978**, *12*, 169.
(69) te Velde, G. *Amsterdam Density Functional ADF, User Guide*, Release 1.1.3; Department of Theoretical Chemistry, Free University: Amsterdam, The Netherlands, 1994.
(70) Ravenek, W. In *Algorithms and Applications on Vector and Parallel Computers*; te Riele, H. J. J., Dekker, T. J., van de Horst, H. A., Eds.; Elsevier: Amsterdam, The Netherlands, 1987.
(71) Krijn, J.; Baerends, E. J. Fit Functions in the HFS Method; Department of Theoretical Chemistry, Free University: Amsterdam, The Netherlands, 1984 {Internal Report (in Dutch)}.
(72) Boerrigter, P. M.; te Velde, G.; Baerends, E. J. *Int. J. Quantum Chem.* **1988**, *33*, 87.
(73) te Velde, G.; Baerends, E. J. *J. Comput. Chem.* **1992**, *99*, 84.
(74) te Velde, G. Ph.D. Thesis, Free University, Amsterdam, The Netherlands, 1990.
(75) Snijders, J. G.; Baerends, E. J.; Vernoijs, P. *At. Data Nucl. Data Tables* **1982**, *26*, 483.
(76) Vernoijs, P.; Snijders, J. G.; Baerends, E. J. Slater Type Basis Functions for the Whole Periodic System; Department of Theoretical Chemistry, Free University: Amsterdam, The Netherlands, 1981 [Internal report (in Dutch)].
(77) Vosko, S. H.; Wilk, L.; Nusair, M. *Can. J. Phys.* **1980**, *58*, 1200.
(78) Becke, A. *Phys. Rev. A* **1988**, *38*, 3098.
(79) Perdew, J. *Phys. Rev. B* **1986**, *33*, 8822.
(80) Perdew, J. *Phys. Rev. B* **1986**, *34*, 7406.
(81) Morton, J. R. *Chem. Rev.* **1964**, *64*, 453.
(82) Shiotani, M. *Magn. Reson. Rev.* **1987**, *12*, 333.
(83) Cunnigham, J. In *Radical Ions*; Kaiser, E. T., Kevan, L., Eds.; John Wiley & Sons: New York, 1968.
(84) Maier, G.; Reisenaur, H. P.; Rohde, B.; Dehnicke, K. *Chem. Ber.* **1983**, *116*, 732.
(85) Herzberg, G. *Spectra of Diatomic Molecules*; van Nostrand Reinhold: New York, 1950.
(86) Greenwood, N. N.; Earnshaw, A. *Chemistry of the Elements*; Pergamon Press: Oxford, New York, 1989.
(87) Versluis, L. Ph.D. Thesis, University of Calgary, Calgary, Alberta, Canada, 1989.
(88) Versluis, L.; Ziegler, T. *J. Chem. Phys.* **1988**, *88*, 322.
(89) Fan, L.; Ziegler, T. *J. Chem. Phys.* **1991**, *95*, 7401.
(90) Schreckenbach, G.; Li, J.; Ziegler, T. *Int. J. Quantum Chem., Quantum Chem. Symp.* **1995**, *56*, 477.
(91) Ziegler, T.; Snijders, J. G.; Baerends, E. J. *J. Chem. Phys.* **1981**, *74*, 1271.
(92) Li, J.; Schreckenbach, G.; Ziegler, T. *J. Phys. Chem.* **1994**, *98*, 4838.
(93) Li, J.; Schreckenbach, G.; Ziegler, T. *J. Am. Chem. Soc.* **1995**, *117*, 486.
(94) Li, J.; Schreckenbach, G.; Ziegler, T. *Inorg. Chem.* **1995**, *34*, 3245.
(95) IGLO stands for the "individual gauge for localized orbitals" method.[96−98]
(96) Kutzelnigg, W. *Isr. J. Chem.* **1980**, *19*, 193.
(97) Schindler, M.; Kutzelnigg, W. *J. Chem. Phys.* **1982**, *76*, 1919.
(98) Kutzelnigg, W.; Fleischer, U.; Schindler, M. In *NMR—Basic Principles and Progress*; Springer-Verlag: Berlin, 1990; Vol. 23, p 165.
(99) Ellis, P. D.; Odom, J. D.; Lipton, A. S.; Chen, Q.; Gulick, J. M. In *Nuclear Magnetic Shieldings and Molecular Structure;* Tossell, J. A., Ed.; NATO ASI Series C, Mathematical and Physical Sciences, 386; Kluwer Academic Publishers: Dordrecht, The Netherlands, 1993; p 539.
(100) Schreckenbach, G.; Ruiz-Morales, Y.; Ziegler, T. *J. Chem. Phys.* **1996**, *104*, 8605.
(101) Magyarfalvi, G.; Pulay, P. *Chem. Phys. Lett.* **1994**, *224*, 280.
(102) van Lenthe, E., 1996, private communication.
(103) Case, D., 1996, private communication.
(104) Wolinski, K.; Hinton, J. F.; Pulay, P. *J. Am. Chem. Soc.* **1990**, *112*, 8251.
(105) van Leeuwen, R.; Baerends, E. J. *Phys. Rev. A* **1994**, *49*, 2421.
(106) van Leeuwen, R.; Gritsenko, O.; Baerends, E. J. *Z. Phys. D* **1995**, *33*, 229.